DNA Crystal Growth

DOI: 10.1002/anie.201103604

Coverage Control of DNA Crystals Grown by Silica Assistance**

Junwye Lee, Sunho Kim, Junghoon Kim, Chang-Won Lee, Yonghan Roh, and Sung Ha Park**

The impetus behind the current interest in combining DNA materials with conventional nanotechnologies, such as nanoelectronics,[1,2] biosensors,[3,4] and nanophotonics,[5,6] emanates from an ambition to exploit its remarkable properties.[7] One of these properties is self-assembly that is driven by the thermodynamics of sticky end hybridization and makes structural DNA nanotechnology a prime candidate for bottom-up fabrication schemes in these fields. However, unless self-assembled DNA nanostructures can be fabricated on solid surfaces to at least the degree of accuracy of existing top-down methods, it will be unfeasible to replace it with existing technologies. An intermediate step toward this goal has been to merge the two approaches such that DNA nanostructures are self-assembled onto lithographically patterned substrates. Previous works have been successful at depositing self-assembled DNA nanostructures on patterned substrates[8,9] and controlling the spatial orientations of tailored DNA origami motifs at specifically designated sites.[10–12] All these approaches have used random depositions (or similar methods) of preformed DNA structures onto lithographically patterned substrates. What has been lacking in literature is a method of precisely controlling the coverage of DNA structures on various substrates, that is, the percentage of the surface covered by crystals, especially on silica (SiO_2), which is crucial if DNA is to be universally employed in electronics. We provide a solution to this problem by introducing a new surface-assisted fabrication method, termed the silica-assisted growth (SAG) method, to self-assemble DNA nanostructures on SiO_2 surfaces. The novel fabrication technique presented herein bears two important distinctions from previous studies. Firstly, direct annealing on the substrates allows for very accurate control of the amount of DNA structures that self-assemble on the substrate, that is, the coverage. Secondly, because of electrostatic interactions with the silica surface, structures grown by this method show drastic topological changes that lead to previously unreported novel structures.

The pretreatment process of SiO_2 substrates and the various DNA structures grown on them are shown in Figure 1. Silanol groups on the SiO_2 surface become deprotonated once the substrates are treated in a $10\times$ TAE/Mg^{2+} buffer (see the Experimental section for details) since the pH of this buffer exceeds the isoelectric point of SiO_2.[13] This approach allows Mg^{2+} ions to bind to the substrate surface, which in turn binds the negatively charged DNA backbones (Figure 1a).[10] To demonstrate the SAG method, four different types of DNA nanostructures were prepared. 8 helix tubes (8 HT) and 5 helix ribbons (5 HR) were constructed from single-stranded tiles (SST),[14] while double-crossover (DX) crystals and DX crystals with biotin modifications were fabricated from DX tiles (see Figure S1–S3 in the Supporting Information).[15] The schematic diagrams of the various DNA structures are illustrated in Figure 1b–f and their corresponding AFM images on SiO_2 substrates are shown in Figure 1g–p (Figure 1g–k show structures made from the free solution annealing method deposited onto SiO_2 for imaging and Figure 1l–p show structures made using the SAG method where the structures are annealed directly on the substrate, see Figure S4 in the Supporting Information).

For the 8 HT, there is a dramatic difference between the structure formations of the free solution annealing method and the SAG method. Caused by a local minimum in the free energy landscape,[14] monodisperse 8 HT structures on SiO_2 fabricated from the free solution annealing method are stable, which can be clearly seen in Figure 1g. In this case, the structures have already been formed in solution before they are deposited onto the substrate. Meanwhile, in the case of SAG, the charges of the Mg^{2+} ions bound on the substrate surface interact with the DNA strands to prevent the formation of tubes. Through these interactions, an acute topological change of the structures occurs, allowing SSTs to bind edgewise and to remain in a single-layer state (Figure 1l) with some of the tiles overlapping along their boundaries (Figure 1l, bright regions). To the best of our knowledge, this is the first observation of 2D crystals arising from SST motifs. Another type of 1D structure, the 5 helix ribbon, was also successfully fabricated using both the free solution annealing and SAG methods as can be seen in Figure 1h and m, respectively. The substrate acts as a catalyst to reduce the amount of energy needed for DNA structures to form, resulting in large-scale structure formations on the substrates.[16]

In the case of DX crystals, two-tile units of DX monomers were used as building blocks to fabricate periodic arrays. One

[*] J. Lee,[+] J. Kim, Prof. S. H. Park
Sungkyunkwan Advanced Institute of Nanotechnology (SAINT) and Department of Physics, Sungkyunkwan University
Suwon 440-746 (Korea)
E-mail: sunghapark@skku.edu
S. Kim,[+] Prof. Y. Roh
School of Information and Communication Engineering, Sungkyunkwan University
Suwon 440-746 (Korea)
E-mail: yhroh@skku.edu
Dr. C.-W. Lee
Samsung Advanced Institute of Technology (SAIT)
Yongin 446-712 (Korea)
[+] These authors contributed equally to this work.

[**] This work was supported by the Joint Research Project under the KOSEF-JSPS Cooperative Program (F01-2009-000-10205-0) to S.H.P and by the National Research Foundation (NRF) of Korea funded by the Korean government (MEST) (No. R01-2008-000-20582-0) to Y.R.
Supporting information for this article is available on the WWW under http://dx.doi.org/10.1002/anie.201103604.

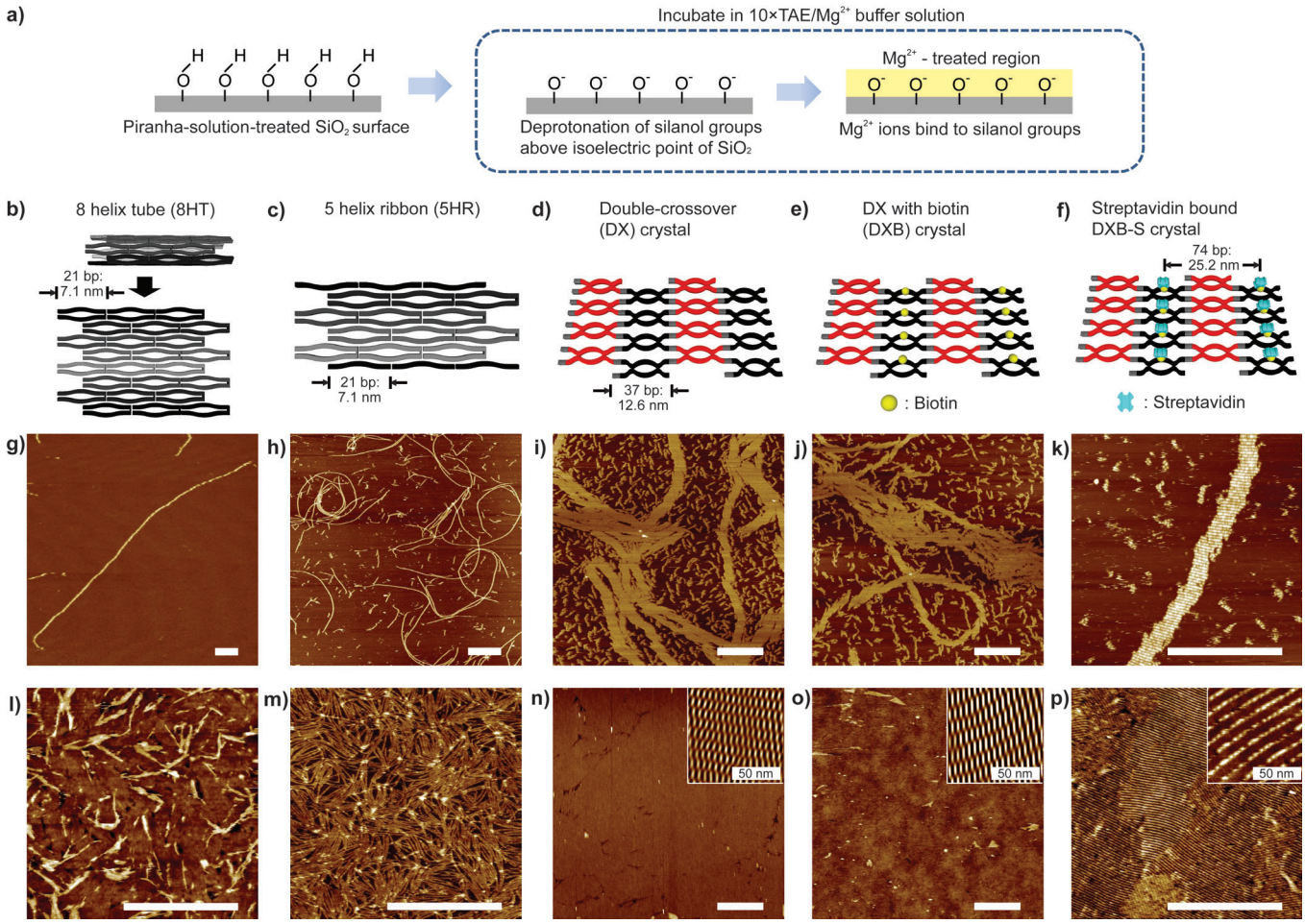

Figure 1. DNA nanostructure fabrication by silica-assisted growth (SAG). a) Pretreatment of SiO_2 substrates in a piranha solution, followed by incubation in a 10×TAE/Mg^{2+} buffer solution. b–f) Schematic diagrams of the various DNA nanostructures made by the free solution annealing and SAG methods; 8 helix tubes (b), 5 helix ribbons (c), double-crossover (DX) crystals (d), double-crossover crystals with biotin (DXB) (e), and streptavidin bound double-crossover (DXB-S) crystals with biotin (f). g–p) AFM images of the structures fabricated by the free solution annealing method (g–k) and the SAG method (l–p). AFM images in the same column as the schematic diagrams of the DNA structures (b–f) correspond to those structures. 8 HT structures, fabricated from an SST motif, in a free solution are 1D crystals (g), but change into 2D polycrystalline structures by using the SAG method (l). Images of DX crystals (n–p) grown by the SAG method show 100% coverage. The insets in (n) and (o) are noise-filtered reconstructed images by fast Fourier transform showing the periodicity of the crystals. The inset in (p) is a magnification of the DX–S crystal. The scale bars in all the AFM images are 1 μm unless otherwise noted.

of the key factors that limits the employment of DNA nanostructures in applications has been the lack of control of the coverage of the various DNA motifs on substrates. For DX crystals grown from the free solution annealing method (Figure 1 i), the crystals prefer to assemble in the longitudinal direction of the tiles, leaving large sections uncovered by crystals. In stark contrast, due to a topological transformation which causes a change in the aspect ratio of the crystal, crystals grown with the SAG method (Figure 1 n) form large domains on the substrate. t Control of the coverage by these domains can be achieved by adjusting the concentration of the DX monomers, [DX] (see Figure S5 in the Supporting Information). Furthermore, as illustrated by the successful fabrication of DX crystals with biotinylated oligonucleotides (DXB), the functionality of the DX crystals remains unchanged when grown with the SAG method (Figure 1 e,j,o). As with ordinary DX crystals, a drastic difference in the coverage between the free solution annealing method (Figure 1 j) and the SAG method (Figure 1 o) was observed. The periodic attachment of the biotin molecules to the DX crystals becomes much more apparent when streptavidin is added to the solution, a protein with a high binding affinity for biotin (see Figure S6 in the Supporting Information). Figure 1 f illustrates a schematic diagram of the DXB crystal containing streptavidin proteins (DXB–S), which can be seen in the AFM images as bright dots for the free solution annealing method (Figure 1 k) and the SAG method (Figure 1 p). In all the experiments concerning DX crystals (DX, DXB, and DXB–S), major topological transformations occurred and exact control of the coverage was possible with the SAG method.

The coverage dependence on the DX monomer concentration for the SAG method was measured by annealing different concentrations of DNA strands (Figure 2).[17] Figure 2 a represents a schematic illustration of the SAG annealing process and Figure 2 b–g show AFM images of

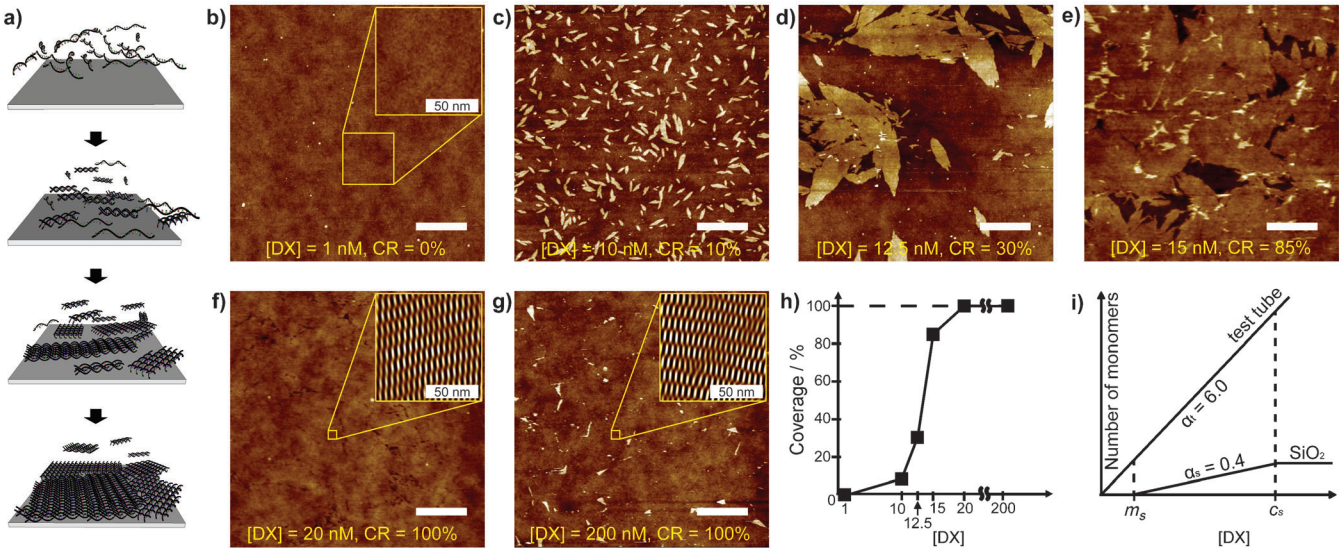

Figure 2. Coverage control by DX monomer concentrations. a) Schematic diagram illustrating the kinetic process of crystal synthesis on a silica substrate. b–g) The coverage of silica can be straightforwardly controlled by increasing the DX monomer concentrations ([DX]). Noise-filtered fast Fourier transform images showing no signs of crystal periodicity (inset of b) and definite crystal periodicity (insets of f and g). h) Plot of the coverage versus the DX monomer concentration. A coverage of 100% is reached at [DX] = 20 nM and persists till 200 nM, which was the highest concentration tested. i) Schematic plot of the number of monomers versus [DX]. The rate of increase of the number of monomers in the test tube ($\alpha_t = 6.0$) is larger than the rate of increase of the number of monomers on the substrate ($\alpha_s = 0.4$) for $m_s \leq [DX] \leq c_s$. This result indicates that higher levels of supersaturation in the solution need to be achieved for crystal growth on the substrate as [DX] is increased. The scale bars in all AFM images are 1 μm unless otherwise noted.

crystal formations with increasing [DX]. Assemblies of DX crystals begin to appear at a threshold concentration of 10 nM (Figure 2c), that is, the monomer saturation concentration (m_s). The actual nucleation of the crystals may begin at a lower concentration than 10 nM, thus implying that ms may be lower than 10 nM, but because of accuracy limitations in the experiment (AFM resolution, deviations in the pipette volume, etc.) we have set ms = 10 nM. As mentioned above, crystals formed on the substrate are topologically different from ordinary free solution DX crystals. The saturation concentration at which the SiO_2 substrate is completely covered by a monolayer of DX crystals is 20 nM (Figure 2f). As with 5 HR and 8 HT, when structures are grown using SAG, the substrate acts to lower the activity, and thus the free energy, as crystallization of DX crystals occurs slightly below 10 nM instead of typical free solution concentrations of approximately 50 nM. The coverage dependence on the concentration is shown in Figure 2h and a schematic diagram of the crystal growth is shown in Figure 2i. As [DX] is increased and passes m_s, the DX tiles start to crystallize on the substrate and continues to grow until a crystal saturation concentration (c_s) is reached, at which point the substrate is fully covered by monolayers of DX crystals. Thus, by controlling [DX], accurate control of the coverage of DX crystals on the substrate is possible, from 0 to 100%.[18]

Another crucial factor in applications of DNA nanostructures is the accurate formation of the structures onto lithographic patterns. Figure 3a shows the patterning process of SiO_2; photoresist (PR) patterns were formed by covering a PR layer deposited on a SiO_2 substrate with a mask and exposing it to UV light. After development, the substrates were dipped in a octadecyltrichlorosilane (OTS) solution.[19] The PR patterns were removed and the substrate was treated in a piranha solution (H_2O_2(30%):H_2SO_4(96%) = 1:2)after which the substrate was incubated in a 10 × TAE/Mg^{2+} buffer solution for deprotonation. This patterned substrate was then used in the SAG annealing process with the intent that DNA structures would only form on the surfaces of the SiO_2 substrate and not on OTS monolayers due to a Coulomb attraction between the DNA strands and regions of the substrate treated with Mg^{2+} ions and the prevention of Mg^{2+} ions binding to the hydrophobic methyl-terminated OTS monolayers (Figure 3a). The binding of Mg^{2+} ions to SiO_2 and not to OTS surfaces can be verified by electric force microscopy (EFM). Untreated OTS monolayers have a higher electric potential compared to SiO_2 surfaces whereas the situation is reversed once SiO_2 is treated with a 10 × TAE/Mg^{2+} buffer solution.[20] Successful patterning of DNA monolayers using this method was confirmed through AFM images (Figure 3b–i). The yellow dashed lines indicate the boundaries between the crystals of the DNA monolayers (dark regions) and the OTS monolayers (bright regions). Line and square patterns of DXB monolayers are shown in Figure 3b,c,d and Figure 3e, respectively, where the accuracy of the DNA growth matching the lithographic patterns can be seen. This observation becomes more conspicuous once streptavidin is added (Figure 3f–i). The bright lines of the crystals in Figure 3g,i are due to DXB crystals, in which streptavidin has been attached (DXB–S). The precision of the DNA growth can be observed in the square patterns (Figure 3h,i), in which the DXB–S crystals have grown to exactly fit the rounded corners of the squares (see Figure S8 in the Supporting Information). Analyses of all the images confirm a very high degree of DNA pattern accuracy.

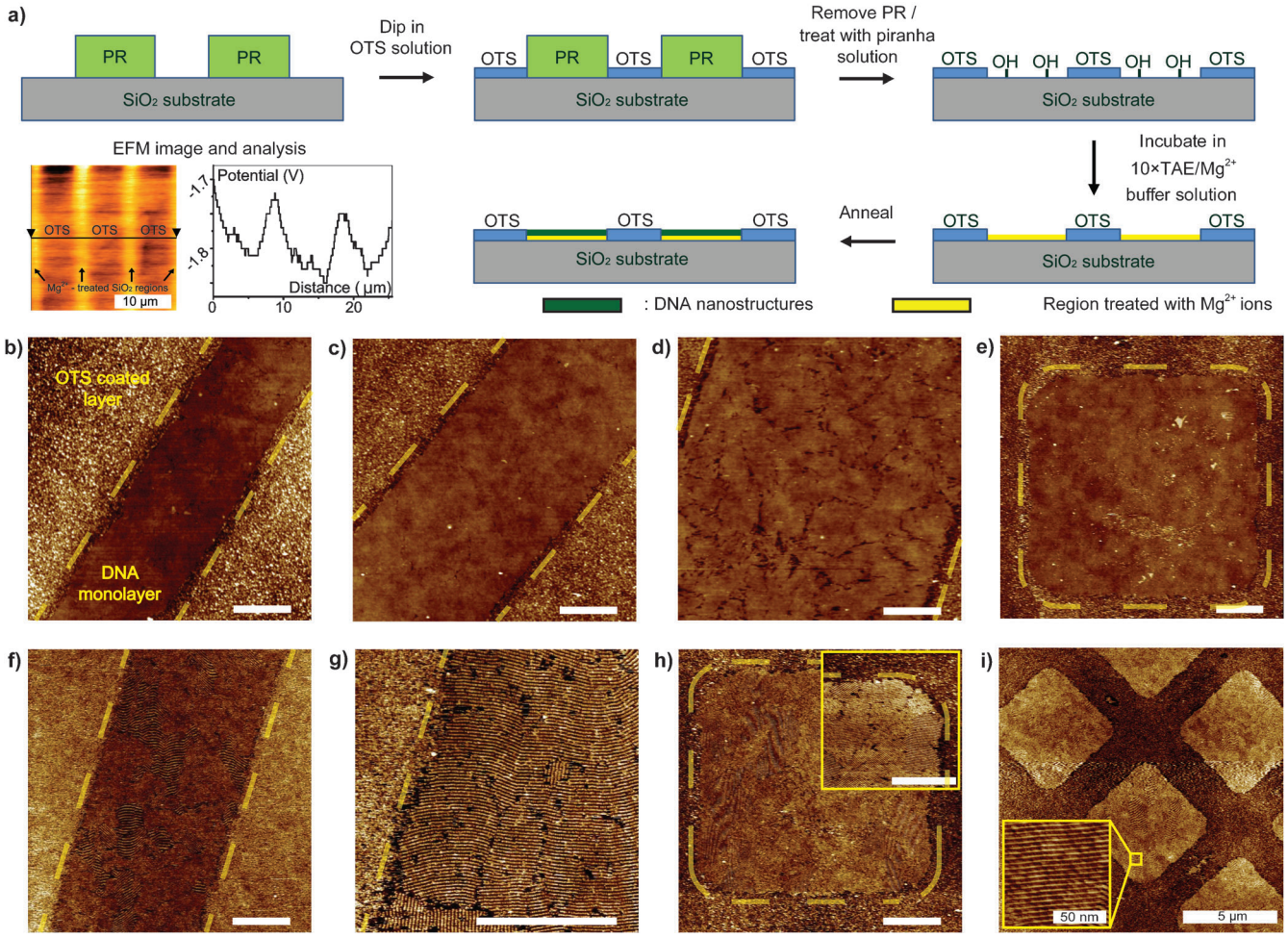

Figure 3. DX crystals grown by silica assistance on patterned silica substrates. a) Process of lithographically patterning SiO_2 substrates. The EFM image verifies regular patterns of potential differences between the embossed (OTS layer) and depressed (deprotonated SiO_2) features of the substrate. b–e) AFM images of a monolayer of DX crystals grown using SAG on a patterned substrate with gap widths of 2 μm (b), 3 μm (c), 5 μm (d), and a square pattern of 5 μm × 5 μm (e). f–i) AFM images of DXB–S crystals grown using SAG on a patterned substrate with gap widths of 3 μm (f), 5 μm (g), a square pattern of 5 μm × 5 μm with the inset showing a magnified image of the corner of the square detailing the intricate growth of the DXB–S crystal (h), and square islands of DXB–S crystals self-assembled on a patterned silica substrate (i). The scale bars in all the AFM images are 1 μm unless otherwise noted and the yellow dashed lines are guides for the eyes.

The range of applications which may benefit from this fabrication scheme seems very broad. SiO_2-integrated nanostructures and devices with novel physical, chemical, and biological properties resulting from the incorporation of DNA are now one step closer to becoming a reality. Biologically templated monolayers for biomolecular sensors,[21,22] DNA monolayers modified with cetyltrimethylammonium to form electron-blocking layers in solar cells,[23] light-emitting diodes,[24,25] host materials in active waveguide structures in electro-optical devices,[26] and gate dielectrics in field-effect transistors[27,28] are just a few examples. Further works to expand the applicability of surface-assisted growth techniques beyond oxide surfaces to metal and polymer surfaces are underway. If successful, these approaches would greatly promote the utility of DNA crystals to almost all types of materials at the micro and nanometer scale.

Experimental Section

Pretreatment of SiO_2 substrates: 300 nm-thick SiO_2 layers were thermally grown on *p*-type silicon substrates. The SiO_2 wafers were cleaned by piranha solution for 30 min, followed by rinsing with deionized water. The cleaned wafers were cut into 0.5×0.5 cm^2 pieces with a diamond tip pen and were immersed into a microtube filled with 1 mL of $10 \times TAE/Mg^{2+}$ buffer solution (400 mM tris(hydroxymethyl)aminomethane (Tris), 10 mM ethylenediaminetetraacetic acid (EDTA; pH 8.0), 125 mM magnesium acetate) for 3 h, followed by rinsing with deionized water.

DNA Annealing: Synthetic oligonucleotides, purified by HPLC, were purchased from Integrated DNA Technologies (IDT, Coralville, IA). Details can be found on www.idtdna.com. Complexes were formed by mixing a stoichiometric quantity of each strand in physiological buffer, $1 \times TAE/Mg^{2+}$. A final concentration of 200 nM is achieved. For annealing, the substrate along with the DNA strands were inserted into AXYGEN tubes which were then placed in a styrofoam box with 2 L of boiled water and cooled slowly from 95 °C to 20 °C over a period of at least 24 h to facilitate the hybridization process.

Streptavidin binding to DX-Biotin Nanostructures: Biotinylated oligos were purchased from www.idtdna.com. Streptavidin was purchased from Rockland Inc. (PA, USA). A 200 nM solution of streptavidin was prepared in deionized water. A 1:1 ratio of streptavidin–SAG DXB was prepared by directly adding streptavidin solution to the test tube.

AFM Imaging: For AFM imaging, a SAG sample was placed on a metal puck using instant glue. 30 μL 1 × TAE/Mg^{2+} buffer was then added onto the substrate and another 5–10 μL of 1 × TAE/Mg^{2+} buffer was dispensed into the AFM tip (Veeco Inc.). AFM images were obtained with a Multimode Nanoscope (Veeco Inc.) in liquid tapping mode.

Preparation process of SiO_2 patterns: 2 μm-thick photoresist (AZ5214) patterns that consist of arrays of lines and squares were formed on the SiO_2 wafers by a photolithography processes. To form an OTS self-assembled monolayer, the wafers were immersed into a solution of OTS (0.1 mM) and hexane for 1 hour. Subsequently, the wafers were immersed and sonicated in acetone to strip photoresist patterns. Residual photoresists were removed and selective hydrophilic patterns were formed by immersing OTS/SiO_2 patterns into a piranha solution for 3 min and rinsing with deionized water. After 3 min of treatment with piranha solution, the OTS regions of the SiO_2 substrates remain hydrophobic whereas the SiO_2 layer turns hydrophilic.

EFM Imaging: For EFM imaging, a patterned silica substrate treated with Mg^{2+} ions was placed on a metal puck using instant glue and was dried using a nitrogen gun. EFM images were obtained by SPA400 AFM (Seiko) with a tip voltage of 10 V and a tip frequency of 23 kHz.

Received: May 26, 2011
Published online: August 26, 2011

Keywords: DNA · DNA structures · self-assembly · silica · streptavidin

[1] E. Braun, Y. Eichen, U. Sivan, G. Ben-Yoseph, *Nature* **1998**, *391*, 775 – 778.
[2] A. Rakitin, P. Aich, C. Papadopoulos, Yu. Kobzar, A. S. Vedeneev, J. S. Lee, J. M. Xu, *Phys. Rev. Lett.* **2001**, *86*, 3670 – 3673.
[3] J. M. Nam, C. S. Thaxton, C. A. Mirkin, *Science* **2003**, *301*, 1884 – 1886.
[4] Y. Lu, B. R. Goldsmith, N. J. Kybert, A. T. C. Johnson, *Appl. Phys. Lett.* **2010**, *97*, 083107.
[5] F. D. Lewis, *Photochem. Photobiol.* **2005**, *81*, 65 – 72.
[6] A. J. Steckl, *Nat. Photonics* **2007**, *1*, 3 – 5.
[7] N. C. Seeman, *Nature* **2003**, *421*, 427 – 431.
[8] K. Sarveswaran, W. Hu, P. W. Huber, G. H. Bernstein, M. Lieberman, *Langmuir* **2006**, *22*, 11279 – 11283.
[9] A. E. Gerdon, S. S. Oh, K. Hsieh, Y. Ke, H. Yan, H. T. Soh, *Small* **2009**, *5*, 1942 – 1946.
[10] R. J. Kershner, L. D. Bozano, C. M. Micheel, A. M. Hung, A. R. Fornof, J. N. Cha, C. T. Rettner, M. Bersani, J. Frommer, P. W. K. Rothemund, G. M. Wallraff, *Nat. Nanotechnol.* **2009**, *4*, 557 – 561.
[11] A. M. Hung, C. M. Micheel, L. D. Bozano, L. W. Osterbur, G. M. Wallraff, J. N. Cha, *Nat. Nanotechnol.* **2010**, *5*, 121 – 126.
[12] B. Ding, H. Wu, W. Xu, Z. Zhao, Y. Liu, H. Yu, H. Yan, *Nano Lett.* **2010**, *10*, 5065 – 5069.
[13] J. P. Brunelle, *Pure Appl. Chem.* **1978**, *50*, 1211 – 1229.
[14] P. Yin, R. F. Hariadi, S. Sahu, H. M. T. Choi, S. H. Park, Th. H. LaBean, J. H. Reif, *Science* **2008**, *321*, 824 – 826.
[15] E. Winfree, F. Liu, L. A. Wenzler, N. C. Seeman, *Nature* **1998**, *394*, 539 – 544.
[16] S. Hamada, S. Murata, *Angew. Chem.* **2009**, *121*, 6952 – 6955; *Angew. Chem. Int. Ed.* **2009**, *48*, 6820 – 6823. The results of the substrate-assisted assembly of this reference differ from the SAG method presented in this study in two ways, namely, the direct control of the coverage and the topological changes of DNA nanostructures.
[17] To achieve a consistent and reliable diagram, three crystal growth conditions, that is, the substrate size (5 mm × 5 mm), the total DNA sample volume (500 μL), and annealing time (ca. 24 h in 2 L of water in a styrofoam box) were fixed, while different DNA monomer concentrations were used as a control parameter.
[18] It should be noted that the crystal growth rate on the substrate (α_s) is smaller than the rate of the increase of monomers in the free solution of the test tube (α_t) by a factor of approximately 1/15, as [DX] is increased from ms to c_s, shown in Figure 2i (Table S1 and Figure S7 in the Supporting Information). Under normal saturation conditions for $m_s \leq [DX] \leq c_s$, α_t should equal α_s, but the fact that α_t is larger than α_s implies that caused by the finite size of the substrate, crystals that have already formed on the substrate prevent newly forming crystals from attaching to it, thus making it necessary to supersaturate the free monomer concentration in the test tube in order to increase the number of crystal formations on the silica substrate.
[19] Y. Wang, M. Lieberman, *Langmuir* **2003**, *19*, 1159 – 1167.
[20] J. J. Shyue, M. R. De. Guire, T. Nakanishi, Y. Masuda, K. Koumoto, C. N. Sukenik, *Langmuir* **2004**, *20*, 8693 – 8698.
[21] E. S. Andersen, M. Dong, M. M. Nielsen, K. Jahn, R. Subramani, W. Mamdouh, M. M. Golas, B. Sander, H. Stark, C. L. P. Oliveira, J. S. Pedersen, V. Birkedal, F. Besenbacher, K. V. Gothelf, J. Kjems, *Nature* **2009**, *459*, 73 – 77.
[22] M. Rahman, M. L. Norton, *IEEE Trans. Nanotechnol.* **2010**, *9*, 539 – 542.
[23] V. Kolachure, M. H. C. Jin, Photovoltaic specialists conference 33rd IEEE, **2008**.
[24] J. A. Hagen, J. G. Grote, W. Li, A. J. Steckl, *Appl. Phys. Lett.* **2006**, *88*, 171109.
[25] Q. Sun, D. W. Chang, L. Dai, J. Grote, R. Naik, *Appl. Phys. Lett.* **2008**, *92*, 251108.
[26] E. M. Heckman, P. P. Yaney, J. G. Grote, F. K. Hopkins, *Appl. Phys. Lett.* **2006**, *89*, 181116.
[27] C. Yumusak, Th. B. Singh, N. S. Sariciftci, J. G. Grote, *Appl. Phys. Lett.* **2009**, *95*, 263304.
[28] Y. S. Kim, K. H. Jung, U. R. Lee, K. H. Kim, M. H. Hoang, J. Jin, D. H. Choi, *Appl. Phys. Lett.* **2010**, *96*, 103307.

